Reconstruction of SWI for Phased Array Head Coil

H. Shen[1,2], G. Cao[3], Z. Tang[2]

[1]GE Healthcare China, Beijing, Beijing, China, People's Republic of, [2]Tsinghua University, Beijing, Beijing, China, People's Republic of, [3]GE Healthcare China, Hongkong, Hongkong, China, People's Republic of

INTRODUCTION

Susceptibility weighted imaging (SWI) has been approved useful in a number of clinical applications, such as seperating arteries and veins[1], imaging high resolution venous vascular network[2], revealing additional information in brain tumor [3], detecting smaller diffuse axonal injury lessions[3], imaging high resolution venous angioma[3], and measuring iron buildup in neurodegenerative diseases[3]. Because multi channel phased array coils are usually the default choice in many routine imaging programs nowadays, it is strongly desirable to be able to implement SWI with phased array coil. In this study we have implementated SWI using 8-channel phased-array head coil and compared two methods to combine the SWI image data from multi channel receivers.

METHOD

Data Acquisition: The datasets used for SWI reconstruction were acquired by a superconductive 3.0T MR scanner (EXCITE II, GEMS, Milwaukee) with an 8-channel phased-array head coil. A 3D GRE pulse squence was employed to acquire axial high resolution images, using the following parameters: TR=28ms, TE=10ms, FA=20°, slice thickness=2~2.5mm, slice gap=0.0mm, FOV=240*240mm², matrix=384*320, NEX=0.75, locs in a slab=28~32.

SWI reconstruction: It is assumed that there is a low-frequency phase component caused by the local field inhomogeneity in original complex images acquired by GRE pulse sequence[1]. To free out the useful phase component from such an effect, one kind of high-pass-filter is employed:

$$\rho_f(x) = \frac{F^{-1}[S(k)]}{F^{-1}[S(k)H(k)]} = \frac{|\rho(x)|e^{i\varphi_h(x)+i\varphi_f(x)}}{|\rho_h(x)|e^{i\varphi_h(x)}} = |\rho_f(x)|e^{i\varphi_f(x)} \quad (1)$$

where *S(k)* is the original k-space data, *H(k)* is a low-pass filter, $\varphi_h(x)$ is the phase component caused by the local field inhomogeneity, $\varphi_f(x)$ is the useful phase component. According to $\varphi_f(x)$, a weighted mask is generated and used on the original magnitude image to get the SWI image. A 32-width low-pass filter was used in this study, and the negtive weighted mask was multiplied 4 times.

Coil sensitivity: At a given spacial location, NMR signal of interest will be detected with different intensity by different element of the phased array coil[5], $S_i = \rho b_i + e_i$, where ρ is the NMR signal of interest, b_i is the sensitivity of the i-th element, e_i is the noise introduced by the i-th elemnet, and S_i is the intensity detected by the i-th element. To get the optimized ρ, the folloing equation will be used:

$$P_{\text{opt}} = \frac{1}{\sum_j b_j^2} \sum_i S_i b_i^* \quad (2)$$

where b_i^* is the complex conjunction of b_i. Since b_i is not usually known for each pixel, there are two alternative methods in practice: Average of Sum (AOS) when $b_i = 1$ and Root of Aquare Sum (RSS) when $b_i = S_i / \sqrt{\sum_k S_k^2}$. In this study, both methods were used to get the combined final SWI image. Matlab was used to analyse the results.

RESULTS AND DISCUSSION

Fig. 1-8 shows the 8 SWI images reconstructed from each coil element of the 8-channel phased array coil. The sensitivity profiles of the 8 elements can be observed different obviously. Fig. 9 is obtained from Fig. 1-8 by AOS. Fig. 10 is obtained by RSS. Fig. 11-12 present the central horizonal and vertical profiles of Fig. 10. Fig. 13-14 present the corresponding profiles of Fig. 11. Table 1 shows some statistic values of the profile segments in the phantom from Fig. 11-14. With the comparison, it is easy to get a conclusion that AOS can reconstruct a more homogenous SWI image than RSS method. Fig. 15-16 show SWI images from a volunteer reconstructed by AOS and RSS. In Fig. 16, it is much darker at center than periphery region, ie. the AOS method gives more uniform signal intensity. Because b_i in assumption is not the exact sensitivity of coil, there are still some kind of inhomogeneity dependent on the sensitivity difference of each coil element. It is worth evaluating the actual b_i of every coil element to get the more uniform result in the future.

Table 1

	Fig. 12	Fig. 13	Fig. 14	Fig. 15
Average	112.5	109.5	124.3	120.6
Max	120	123	144	155
Min	106	85	114	99
SD	3.2	11.3	7.1	14.7

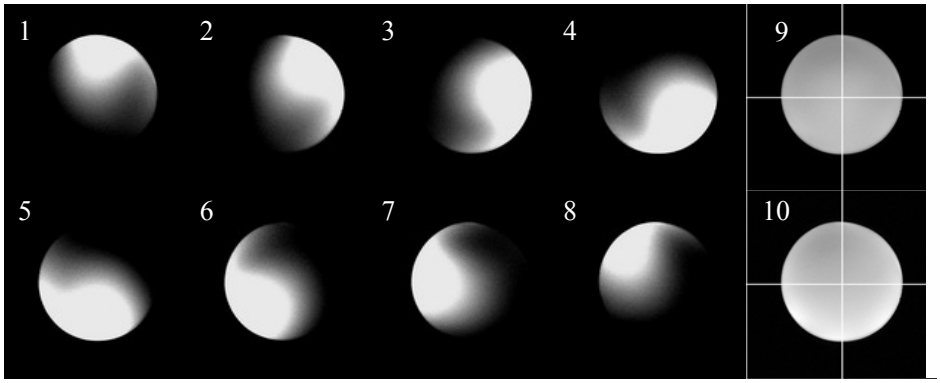

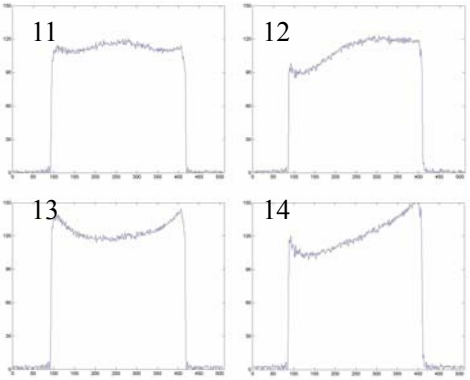

Fig. 1-8: Phantom's SWI images from each coil component of 8-channel phased array coil.
Fig. 9: Final SWI image combined by AOS. **Fig. 11:** Final SWI image combined by RSS.
Fig. 11-12: Profiles of central horizontal and vertical lines in Fig. 10.
Fig. 13-14: Profiles of central horizontal and vertical lines in Fig. 11.
Fig. 15-16: AOS & RSS SWI images of the same volunteer with the same window width and window level.

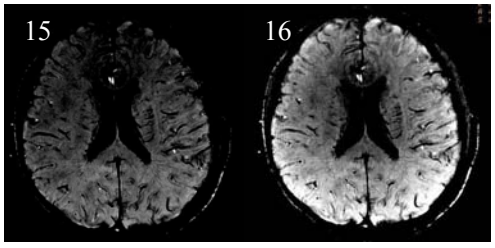

REFERENCES

[1] Wang Y, et al. JMRI, 2000, 12:661-670
[2] Haache E M, et al. MRM, 2004, 52:612-618
[3] Sehgal V, et al. JMRI, 2005, 22:439-450
[4] Pruessmann K P, et al. MRM, 1999, 42:952-962
[5] Bydder M, et al. MRM, 2002, 47:539-538